THE ANNALS OF "DUNĂREA DE JOS" UNIVERSITY OF GALAȚI
FASCICLE V, TECHOLOGIES IN MECANICAL ENGINEERING, ISSN 1221-4566
2005

Algorithm for Hypoid Gear Study

Prof. PhD. eng. Nicolae OANCEA,Stud. Clara PANAIT,Eng. Virgil TEODOR,
„Dunarea de Jos" University of Galati, Faculty of Mechanical Engineering

ABSTRACT

This paper suggests a model, with general character, to study reciprocal wrapped surfaces, by using basic and complementary theorems of wrapping surfaces. By its particularizations, the model can be considered as representing a multitude of known types of gears: worm gear, hypoid gear.
***Keywords**: wrapping surfaces, crossed axis gears.*

1. Introduction

There are known, accepted and applied basic methods (Olivier, Gohman, Willis theorems), to study gear's teeth profiles. Complementary methods, [3], are also applied: "Substituting circles method", "Minimum distance method", "Plane trajectories method". Crossed axis gear can be considered as a "general" type of worm gear that transmits rotation motion between two disjunctive axes.

This paper shows a model, with general character, for the study of reciprocal enwrapping surfaces, by using basic and complementary theorems of wrapping surfaces. By its particularizations, the model can be considered as representing a multitude of known types of gears: worm gear, hypoid gear, parallel axis gear, conical gear etc.

2. Crossed Axis Gear. Reference Systems

In figure 1, there are two axes (Δ_1 and Δ_2) that transmit the rotation motion, by keeping a constant transmission ratio, are presented.

As a general form the studied gear is a hypoid gear for which there are defined:

- xyz is the fixed reference system joined with the plane worm wheel, with the z axis over posed to Δ_1 axis;

-XYZ- mobile reference system joined with the plane worm wheel;

-$x_0y_0z_0$- fixed reference system, joined with the Δ_2 (Y_1) axis of the hypoid worm;

-$X_1Y_1Z_1$- mobile reference system, joined with the worm.

The worm's flank is considered known, which, in general case, is thought as a conical one with its axis different from the plane worm wheel's axis

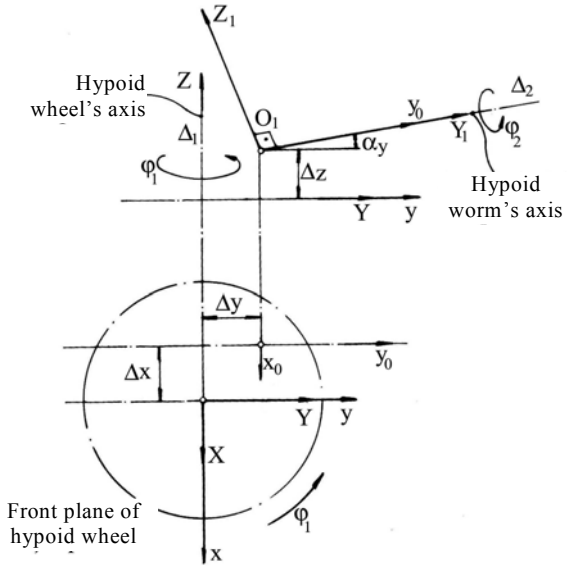

Fig. 1 – Reference Systems; Δ_1 and Δ_2 Rotation Motion Axis

3. The kinematics of the plane worm wheel's flank generation process

Related to the reference systems, shown in Fig.1, there are defined:

-the absolute motion of the XYZ system, as a rotation around Δ_1 axis, by the angular parameter φ_1,

$$x = \omega_3^T(\varphi_1)\cdot X\,; \qquad (1)$$

-the worm's rotation motion around Δ_2 (Y_1) axis, by the angular parameter φ_1,

$$x_0 = \omega_3^T(\varphi_1)\cdot X_1\,; \qquad (2)$$

-coordinates transformation between the xyz and $x_0y_0z_0$ reference systems,

$$x_0 = \beta(x - A)\,, \qquad (3)$$

where:

$$\beta = \begin{Vmatrix} 1 & 0 & 0 \\ 0 & \cos\alpha_y & \sin\alpha_y \\ 0 & -\sin\alpha_y & \cos\alpha_y \end{Vmatrix} \quad (4)$$

is the orthogonal transformation matrix between fix systems (xyz and $x_0y_0z_0$) unitary vectors;

$$A = \begin{Vmatrix} \Delta x \\ \Delta y \\ \Delta z \end{Vmatrix} \quad (5)$$

is the matrix formed by O_1 origin co-ordinates referred to fix system xyz.

NOTE The Δx, Δy, Δz values together with α_y angle are considered as constants, having specific values for each analyzed case.

The absolute motions, (1) and (2), allow finding relative motions – motions between the mobile reference systems.

Thus, from (3), the relative motion results,

$$X = \omega_3(\varphi_1)\left[\beta^T \cdot \omega_2^T(\varphi_2)\cdot X_1 + A\right], \quad (6)$$

representing current point of the space associated to the generalized worm ($X_1Y_1Z_1$ system) referred to the plane worm wheel (XYZ system).

Also, from (6), inverse motion, defined as XYZ space motion toward the $X_1Y_1Z_1$ system, can be determined,

$$X_1 = \omega_3(\varphi_1)\left[\beta^T \cdot \omega_2^T(\varphi_2)\cdot X_1 - A\right]. \quad (7)$$

If in transformation (6) the X_1 matrix means a matrix whose elements represent the worm's flank, then, after developing, the obtained parametrical equations will have the signification of the surfaces family generated by the worm's flank, toward the plane worm wheel's system.

Obviously, transmission ratio,

$$i = \frac{\varphi_2}{\varphi_1}, \quad (8)$$

is considered as constant.

4. The Main Equations of the Worm's Flank

In the reference system $X_1Y_1Z_1$, see figure 1, system over posed, initially, with the fixed reference system $x_0y_0z_0$, (y_0 – worm axis), is defined the worm's axial section is defined (as it can be seen in Fig. 2). Worm is presumed to be a conical one, with $\vec{j}$ as axis and having the helical parameter p, constant).

The current point radius can be defined as

$$r_{b_\theta} = r_{rm} + a_1 \cdot \theta, \quad (9)$$

a_1 means conical spiral parameter and θ – the variable angular parameter.

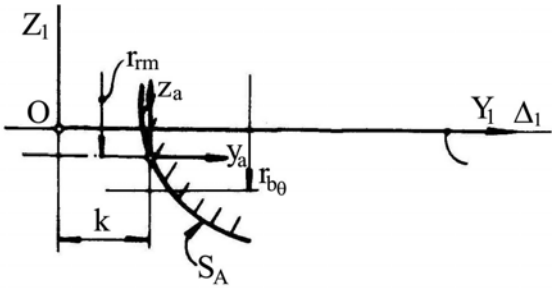

Fig. 2. Worm's axial section

Thus, in the $x_0y_0z_0$ reference system, for the worm's axial section is accepted as:

$$S_A \begin{cases} x_a = 0; \\ y_a = y_a(t) + k; \\ z_a = z_a(t) + r_{b_\theta}, \end{cases} \quad (10)$$

with t independent variable.

In the next motion, the worm's axial profile generates the worm's helical profile

$$\begin{Vmatrix} X_1 \\ Y_1 \\ Z_1 \end{Vmatrix} = \omega_2^T(\theta)\, x_a + p\theta\vec{j}, \quad (11)$$

in which the next definition is obvious

$$x_a = \begin{Vmatrix} 0 \\ y_a(t) \\ z_a(t) \end{Vmatrix}. \quad (12)$$

From (11) and (12), after replacement, it results

$$\begin{Vmatrix} X_1 \\ Y_1 \\ Z_1 \end{Vmatrix} = \begin{Vmatrix} \cos\theta & 0 & \sin\theta \\ 0 & 1 & 0 \\ -\sin\theta & 0 & \cos\theta \end{Vmatrix} \cdot \begin{Vmatrix} 0 \\ y_a(t)+k \\ z_a(t)+r_{b_\theta} \end{Vmatrix} + \begin{Vmatrix} 0 \\ p\theta \\ 0 \end{Vmatrix}. \quad (13)$$

It is developed as:

$$(\Sigma) \begin{cases} X_1 = \left[z_a(t) + r_{b_\theta}\right]\sin\theta; \\ Y_1 = \left[y_a(t) + k\right]\cdot p\theta; \\ Z_1 = \left[z_a(t) + r_{b_\theta}\right]\cos\theta, \end{cases} \quad (14)$$

representing a conical right worm, with t and θ parameters.

5. The Worm Wheel's Flank. The Family of Surface Generated by the Conical Worm in the Wheel's Reference System

From (6) and (14), after replacing the matrix previously defined, the following form results

$$\left\|\begin{matrix}X\\Y\\Z\end{matrix}\right\| = \left\|\begin{matrix}\cos\varphi_1 & \sin\varphi_1 & 0\\ -\sin\varphi_1 & \cos\varphi_1 & 0\\ 0 & 0 & 1\end{matrix}\right\| \cdot \left[\left\|\begin{matrix}1 & 0 & 0\\ 0 & \cos\alpha_y & -\sin\alpha_y\\ 0 & \sin\alpha_y & \cos\alpha_y\end{matrix}\right\| \cdot \left\|\begin{matrix}\cos\varphi_2 & 0 & \sin\varphi_2\\ 0 & 1 & 0\\ -\sin\varphi_2 & 0 & \cos\varphi_2\end{matrix}\right\| \cdot \left\|\begin{matrix}X_1\\Y_1\\Z_1\end{matrix}\right\| + \left\|\begin{matrix}\Delta x\\ \Delta y\\ \Delta z\end{matrix}\right\|\right]. \quad (15)$$

In principle, below equations, (16), is representing family of worm flanks toward the plane wheel's system,

$$(\Sigma)_{\varphi_1}: \begin{vmatrix} X = A(t,\theta,\varphi_2)\cos\varphi_1 + B(t,\theta,\varphi_2)\sin\varphi_1; \\ Y = -A(t,\theta,\varphi_2)in\varphi_1 + B(t,\theta,\varphi_2)\cos\varphi_1; \\ Z = C(t,\theta,\varphi_2). \end{vmatrix} \quad (16)$$

In the equations of family (16), the functions $A(t,\theta,\varphi_2)$, $B(t,\theta,\varphi_2)$, $C(t,\theta,\varphi_2)$ have the following expressions:

$$\begin{aligned} &A(t,\theta,\varphi_2) = X_1(t,\theta)\cos(i\varphi_1) + \\ &Z_1(t,\theta)\sin(i\varphi_1) - \Delta x; \\ &B(t,\theta,\varphi_2) = X_1(t,\theta)\sin(i\varphi_1)\sin\alpha_y + \\ &+Y_1(t,\theta)\cos\alpha_y - Z_1(t,\theta)\cos(i\varphi_1)\sin\alpha_y + \Delta y; \\ &C(t,\theta,\varphi_2) = -X_1(t,\theta)\sin(i\varphi_1)\cos\alpha_y + \\ &+Y_1(t,\theta)\sin\alpha_y + Z_1(t,\theta)\cos(i\varphi_1)\cos\alpha_y + \Delta z. \end{aligned} \quad (17)$$

In principle, the family is represented by equations:

$$(\Sigma)_{\varphi_1} \begin{vmatrix} X = X(t,\theta,\varphi_1); \\ Y = Y(t,\theta,\varphi_1); \\ Z = Z(t,\theta,\varphi_1). \end{vmatrix} \quad (18)$$

6. The Enwrapping Condition

The enwrapping condition, associated to the surfaces family $(\Sigma)_{\varphi_1}$, (18), according to the Gohman's theorem, has the form

$$\vec{N}_\Sigma \cdot \vec{R}_{\varphi_1} = 0, \quad (19)$$

where:

- $\vec{N}_\Sigma$ is the normal to the conical worm flanks surface (14),

$$\vec{N}_\Sigma = \begin{vmatrix} \vec{i} & \vec{j} & \vec{k} \\ X'_{1\theta} & Y'_{1\theta} & Z'_{1\theta} \\ X'_{1t} & Y'_{1t} & Z'_{1t} \end{vmatrix}; \quad (20)$$

- R_{φ_1} is the matrix associated to the vector having the same direction with the speed into the relative motion of the current point belonging to the worm wheel's system toward the worm space,

$$R_{\varphi_1} = \frac{dX_1}{d\varphi_1}. \quad (21)$$

From (6), it results

$$\begin{aligned} R_{\varphi_1} &= \dot{\omega}_2(\varphi_2)\frac{d\varphi_2}{d\varphi_1}\beta\left[\omega_3^T(\varphi_1)X - A\right] + \\ &+\omega_2(\varphi_2)\beta\left[\dot{\omega}_3^T(\varphi_1)X - \frac{dA}{d\varphi_1}\right] \end{aligned} \quad (22)$$

or after the replacement of the X matrix with the (6) form and taking into account the (8) form results

$$\begin{aligned} R_{\varphi_1} &= \dot{\omega}_2(\varphi_2)\frac{d\varphi_2}{d\varphi_1}\beta\left\{\omega_3^T(\varphi_1)\omega_3(\varphi_1)\cdot\right. \\ &\cdot\left[\beta^T\omega_2^T(\varphi_2)X + A\right] - A\Big\} + \\ &+\omega_2(\varphi_2)\beta\left\{\dot{\omega}_3^T(\varphi_1)\omega_3(\varphi_1)\cdot\right. \\ &\cdot\left.\left[\beta^T\omega_2^T(\varphi_2)X + A\right] - \frac{dA}{d\varphi_1}\right\}. \end{aligned} \quad (23)$$

After development, it results the form

$$R_{\varphi_1} = MX_1 + N \quad (24)$$

where:

$$\begin{aligned} M &= i\dot{\omega}_2(\varphi_2)\omega_2^T(\varphi_2) + \\ &+\omega_2(\varphi_2)\beta\dot{\omega}_3^T(\varphi_1)\omega_3(\varphi_1)\beta^T\omega_2^T(\varphi_2) \end{aligned} \quad (25)$$

and

$$N = \omega_2(\varphi)\beta\dot{\omega}_3^T(\varphi_1)\omega_3(\varphi_1)A. \quad (26)$$

After replacements and developments, it is obtained:

$$M = \left\|\begin{matrix} 0 & -\cos\varphi_2\cos\alpha_y & -(i-\sin\alpha_y) \\ \cos\varphi_2\cos\alpha_y & 0 & \sin\varphi_2\cos\alpha_y \\ (i-\sin\alpha_y) & -\sin\varphi_2\cos\alpha_y & 0 \end{matrix}\right\|; \quad (27)$$

$$N = \left\|\begin{matrix} -\Delta x\sin\varphi_2\sin\alpha_y - \Delta y\cos\varphi_2 \\ -\Delta x\cos\alpha_y \\ \Delta x\cos\varphi_2\sin\alpha_y - \Delta y\sin\varphi_2 \end{matrix}\right\|. \quad (28)$$

Thus, the $\vec{R}_{\varphi_1}$ vector is:

$$\begin{aligned}\vec{R}_{\varphi_1} = &\left\{-Y_1(t,\theta)\cos\varphi_2\cos\alpha_y - \right.\\ &-Z_1(t,\theta)\left[i-\sin\alpha_y\right]-\Delta x\sin\alpha_y\sin\varphi_2 - \\ &\left.-\Delta y\cos\varphi_2\right\}\cdot\vec{i}+\left\{X_1(t,\theta)\cos\varphi_2\cos\alpha_y+\right.\\ &\left.+Z_1(t,\theta)\sin\varphi_2\cos\alpha_y-\Delta x\cos\alpha_y\right\}\cdot\vec{j}+\\ &+\left\{X_1(t,\theta)\left[i-\sin\alpha_y\right]-Y_1(t,\theta)\sin\varphi_2\cos\alpha_y\right.\\ &\left.+\Delta x\sin\alpha_y\cos\varphi_2-\Delta y\sin\varphi_2\right\}\cdot\vec{k}\end{aligned} \quad (29)$$

From (19), (20), (29), in principle, a function with following form is determinate

$$q(t,\theta,\varphi_1)=0\,, \quad (30)$$

or, by eliminating one of the variable parameters, the condition becomes

$$t=t(\theta,\varphi_1)\,. \quad (31)$$

The enwrapping surface (the plane wheel's tooth flank) can be expressed through the equations

$$(S):\begin{vmatrix}X=X(\theta,\varphi_1);\\ Y=Y(\theta,\varphi_1);\\ Z=Z(\theta,\varphi_1).\end{vmatrix} \quad (32)$$

Obviously, the representation of the surface S can be done by plane sections, normal on the wheel's axis,

$$Z(\theta,\varphi_1)=H\,, \text{(H random variable).} \quad (33)$$

NOTE For the particularly (single) cases, complementary methods for the enwrapping surfaces can be easy applied.

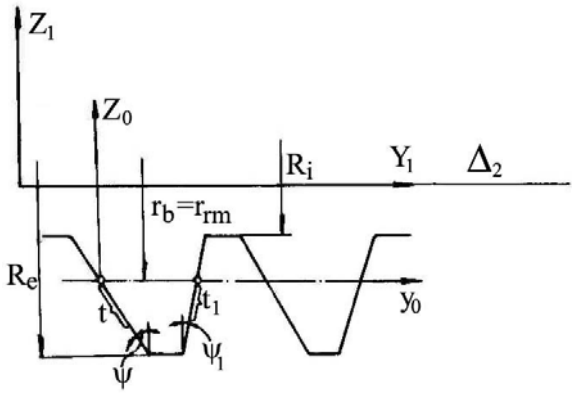

Fig. 3. Hypoid cylindrical worm's axial section

According to the (10) relations and figure 3, the cylindrical worm's axial section is defined:

-for the left flank,

$$S_A:\begin{vmatrix}x_a=0;\\ y_a=t\sin\psi;\\ z_a=-t\cos\psi;\end{vmatrix} \quad (34)$$

-and, similarly, for the right flank,

$$S_A:\begin{vmatrix}x_a=0;\\ y_a=k_0-t_1\sin\psi_1;\\ z_a=-t_1\cos\psi_1.\end{vmatrix} \quad (35)$$

Based on (13) equations, the helical flanks are determined by the following equation considering the (35) relation:

- the left flank,

$$\Sigma_{st}:\begin{vmatrix}X_1=\left[-t\cos\psi-r_{rm}\right]\sin\theta;\\ Y_1=t\sin\psi-p\theta;\\ Z_1=\left[-t\cos\psi-r_{rm}\right]\cos\theta;\end{vmatrix} \quad (36)$$

-the right flank,

$$\Sigma_{dr}:\begin{vmatrix}X_1=\left[-t_1\cos\psi_1-r_{rm}\right]\sin\theta;\\ Y_1=t_1\sin\psi_1+k_0-p\theta;\\ Z_1=\left[-t_1\cos\psi_1-r_{rm}\right]\cos\theta,\end{vmatrix} \quad (37)$$

with $k_0=\dfrac{m\pi}{2}$ wheel's module and p-helical parameter.

7. Modeling Algorithm for the Helical Teeth Wheel's Flank

For this certain case, it may simplify the algorithm by considering the cylindrical worm's rotation motion is equal to the translation motion.

In this way, for the reference systems equivalent to those defined in figure 1, the absolute motions are:

$$x=\omega_3^T(\varphi_1)X\,, \quad (38)$$

meaning the wheel rotation;

$$x=X_1+a;\quad a=\begin{Vmatrix}-\Delta x\\ \Delta y-p\varphi_2\\ r_{rm}\end{Vmatrix}, \quad (39)$$

representing the cylindrical worm's translation.

The relative motion between the mobile reference systems is

$$X=\omega_3(\varphi_1)\left[X_1+a\right] \quad (40)$$

also the inverse motion

$$X_1=\omega_3^T(\varphi_1)X-a \quad (41)$$

NOTE The motion described by the (40) transformation comes from (6) relation for $\varphi_2=0$, $\beta=I^*$ and $A=a$, see(39).

From (40), is determined the worm's surface family in the wheel's reference system,

$$\begin{Vmatrix}X\\ Y\\ Z\end{Vmatrix}=\begin{Vmatrix}\cos\varphi_1 & \sin\varphi_1 & 0\\ -\sin\varphi_1 & \cos\varphi_1 & 0\\ 0 & 0 & 1\end{Vmatrix}\left[\begin{Vmatrix}X_1\\ Y_1\\ Z_1\end{Vmatrix}+\begin{Vmatrix}-\Delta x\\ \Delta y-p\varphi_2\\ r_b\end{Vmatrix}\right]. \quad (42)$$

So, after the equation's development, results

$$(\Sigma)_{\varphi_1}: \begin{vmatrix} X = [X_1 - \Delta x]\cos\varphi_1 - [Y_1 - \Delta y - p\varphi_2]\sin\varphi_1; \\ Y = [X_1 - \Delta x]\sin\varphi_1 + [Y_1 - \Delta y - p\varphi_2]\cos\varphi_1; \\ Z = Z_1 + r_b. \end{vmatrix} \quad (43)$$

The enwrapping condition presumes knowing the Σ surface's normal, which from (36) is calculated as

$$\vec{N}_{\Sigma_{st}} = \begin{vmatrix} \vec{i} & \vec{j} & \vec{k} \\ [-t\cos\psi - r_b]\cos\theta & p & -[-t\cos\psi - r_b]\sin\theta \\ -\cos\psi\sin\theta & \sin\psi & -\cos\psi\cos\theta \end{vmatrix}, \quad (44)$$

which permits establishing the parameters:

$$\begin{aligned} N_{X_{1st}} &= -p\cos\psi\cos\theta + [-t\cos\psi - r_b]\sin\theta\sin\psi; \\ N_{Y_{1st}} &= [-t\cos\psi - r_b]\cos\psi; \\ N_{Z_{1st}} &= p\cos\psi\sin\theta + [-t\cos\psi - r_b]\cos\theta\sin\psi. \end{aligned} \quad (45)$$

Similar, is defined the right flank's parameters of the normal:

$$\begin{aligned} N_{X_{1dr}} &= -p\cos\psi_1\cos\theta + [-t_1\cos\psi_1 - r_b]\sin\theta\sin\psi_1; \\ N_{Y_{1dr}} &= [-t_1\cos\psi_1 - r_b]\cos\psi_1; \\ N_{Z_{1dr}} &= p\cos\psi_1\sin\theta + [-t_1\cos\psi_1 - r_b]\cos\theta\sin\psi_1. \end{aligned} \quad (46)$$

The "speed" vector in relative motion of the plane wheel's system toward the cylindrical worm's system is defined as

$$R_{\varphi_1} = \frac{dX_1}{d\varphi_1} \quad (47)$$

From (41) transformation is defined

$$R_{\varphi_1} = \dot{\omega}_3^T(\varphi_1)\,\omega_3(\varphi_1)[X_1 + a] - \dot{a} \quad (48)$$

which, after replacing and partial developments, are

$$R_{\varphi_1} = \begin{Vmatrix} 0 & -1 & 0 \\ 1 & 0 & 0 \\ 0 & 0 & 0 \end{Vmatrix} \begin{Vmatrix} X_1 - \Delta x \\ Y_1 + \Delta y - p\varphi_2 \\ Z_1 + r_b \end{Vmatrix} + \begin{Vmatrix} 0 \\ p \\ 0 \end{Vmatrix} \frac{d\varphi_2}{d\varphi_1}. \quad (49)$$

Finally, is expressed as

$$R_{\varphi_1} = \begin{Vmatrix} -Y_1 - \Delta y + p\varphi_2 \\ X_1 - \Delta z + p\dfrac{d\varphi_2}{d\varphi_1} \\ 0 \end{Vmatrix}. \quad (50)$$

The equations (44), (45), (50), taken into account the worm's flank definition (36) or (37), based on the general Gohman's theorem

$$\vec{N}_\Sigma \cdot \vec{R}_{\varphi_1} = 0 \quad (51)$$

determinate the enwrapping condition

$$[-Y_1 - \Delta y + p\varphi_2]N_{X_1} + \left[x_1 - \Delta z + p\frac{d\varphi_2}{d\varphi_1}\right]N_{Y_1} = 0 \quad (52)$$

In the (52) relation, N_{X_1}, N_{Y_1} are the parameters of the normal to both helical surfaces of the flanks.

Finally, the enwrapping condition has a form similar with (30) relation.

The enwrapped surface (S-wheel teeth's flank) is expressed in XYZ system through (43) equation together with the (52) condition.

For more simple graphical representation the plane wheel's flank line are defined in plane sections,

$$Z = H \ \ (H - arbitrar\,var\,iable). \quad (53)$$

In this case, from (43) and (36), results

$$[-t\cos\psi - r_{rm}]\cos\theta + r_b = H, \ \ (H - var\,iable). \quad (54)$$

7. Applications

In figure 4, hypoid worm's profiles are represented in normal plane on the wheel's axis.

In tables 1 and 2, there are shown the co-ordinates of the hypoid worm's profiles, in Z=H planes, for: R_e=20.46 mm; R_i=15.45 mm; p=1.25 mm.

Table 1. Hypoid worm profile –right flank

H [mm]	X_1 [mm]	Y_1 [mm]
-15.46000	13.40149	2.36274
-15.46000	6.79665	3.69433
-15.46000	3.36305	4.22995
-15.46000	1.77317	4.42463
-15.46000	0.21947	4.57636
-15.46000	- 6.27922	4.74830
-15.46000	-10.25766	4.49832
-15.46000	-12.65104	4.24222
-17.96000	9.80051	2.63108
-17.96000	7.58330	3.01442
-17.96000	3.63178	3.57824
-17.96000	-0.00854	3.92559
-17.96000	-1.81063	4.02621
-17.96000	4.49555	2.97857
-19.96000	3.25251	3.11697
-19.96000	-0.96819	3.44369
-19.96000	-2.78163	3.51081
-19.96000	-4.01428	3.53044

Table 2. Hypoid worm profile –left flank

H [mm]	X_1 [mm]	Y_1 [mm]
-19.96000	4.49555	1.16558
-19.96000	3.45775	1.11111
-19.96000	2.43778	1.08766
-19.96000	1.43021	1.09411
-19.96000	0.42984	1.12975
-19.96000	-1.56945	1.28763
-19.96000	-2.57843	1.41027
-17.96000	-3.60054	1.56296
-17.96000	9.80051	0.81809
-17.96000	5.54633	0.10848
-17.96000	1.79339	-0.07287
-17.96000	-1.81063	0.17812
-15.46000	-5.56503	0.86167
-15.46000	13.40149	0.54975
-15.46000	8.73303	-0.76042
-15.46000	5.02387	-1.37606
-15.46000	1.77317	-1.52675
-15.46000	-4.54292	-0.70808
-15.46000	-8.16306	0.33189
-15.46000	-12.65104	2.02077

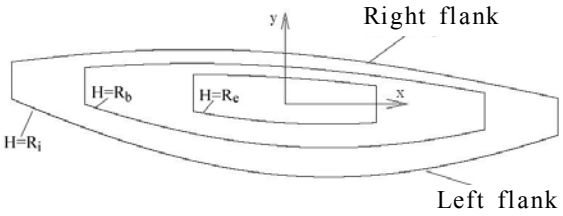

Fig. 4. In-plane sections of the hypoid worm

NOTE The hypoid worm's profiles, in Z=H planes, were drew for the variation limits of t and t_1 parameter, see equation (36) and (37):

-for the left flank,

$$t = \frac{h - r_b \cos\theta}{\cos\theta \cos\psi}; \qquad (55)$$

-for the right flank,

$$t_1 = \frac{h - r_b \cos\theta}{\cos\theta \cos\psi_1}. \qquad (56)$$

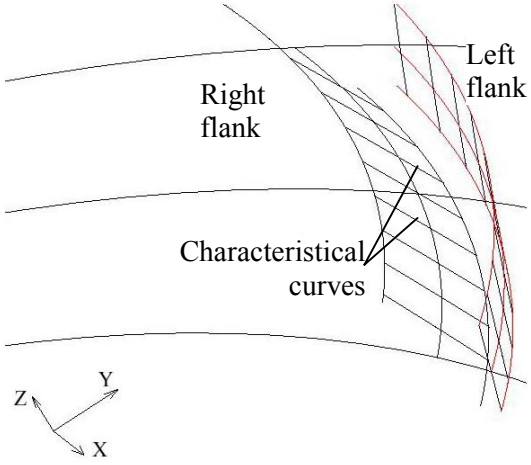

Fig. 5. The hypoid wheel flank's surfaces

For the worm's profiles presented (see figure 4 and tables 1 and 2) based on the established algorithm in the 7.1 paragraph, were determined:

-the hypoid wheel's flanks (see Fig. 2)

-the characteristic curves, equation (43), condition (52) and f_1=constant;

-the profiles lines of the hypoid wheel in normal planes on the wheel (equation (43), (52) and (54)).

In table 3, are presented the profiles lines' co-ordinates and the characteristic curves' coordinates.

Table 3.

The profiles lines		
Right flank		
X [mm]	**Y [mm]**	**Z [mm]**
-35.2079	64.1251	-3.0224-
-35.4703	64.4510	2.0454
-35.4567	64.4559	-1.9968
-35.7222	64.7820	-1.0197
-45.6492	68.1977	0.0367
-35.2955	65.0351	1.0350
-34.6282	64.9439	2.0152
-33.9386	64.8478	3.0445
Left flank		
-35.2079	66.4889	-3.0239
-35.4703	66.0123	-2.0293
-35.4567	65.9671	-1.9514
-35.7222	65.5145	-1.0085
-45.6492	64.9900	0.0471
-35.2955	64.3133	1.0425
-34.6282	63.6398	2.0208
-33.9386	62.9532	3.0080

Table 4.

The left characteristic curves					
$\varphi_2 = 0$			$\varphi_2 = \pi$		
-53.7984	63.2809	3.7282	-49.8094	62.829	3.7272
-53.8059	63.3317	3.6415	-49.8104	62.834	3.7185
…	…	…	-49.8071	62.839	3.7099
-53.9848	64.6522	1.3799	…	…	…
-53.9865	64.6523	1.3799	-49.8697	63.655	2.3238
-53.9882	64.6575	1.3712	-49.8678	63.660	2.3152
…	…	….	….	….	….
-54.2859	67.2601	-3.1042	-50.0324	66.819	-3.0854
-54.2881	67.2602	-3.1042	-50.0344	66.825	-3.0940
-54.2860	67.2651	-3.1129	-50.0342	66.830	-3.1027

In figure 6, there is a 3d view of the hypoid wheel's teeth.

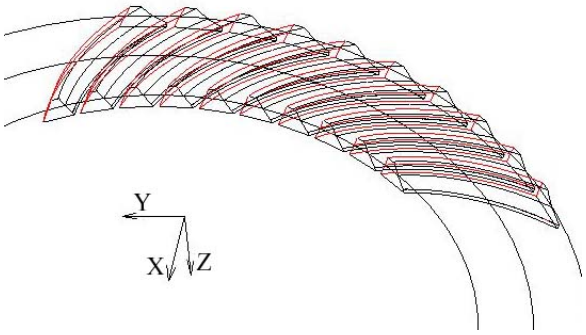

Fig.6. The hypoid wheel's teeth

8. Conclusions

The suggested model allows, by particularizing, studying a wide range of crossed axis gears. The model, developed on the base of both enveloped surfaces general theory and complementary theorems, has the capability to rigorously describe teeth flanks profiles for gearing elements.

Bibliography

1. Boloş, C., Boloş, V., *Elmente privind cinematica de danturare a roţilor melcate spiroide conice*. În: Buletinul ştiinţific al Universităţii Tehnice din Tg. Mureş, vol. VI, 1993, p. 173-178.

2. Litvin, F. L. *Theory of Gearing***,** NASA Reference Publication, Washington, D.C. 1984.

3. O a n c e a N., *Generarea suprafeţelor prin înfăşurare. Vol II – Teoreme complementare*. Ed. Fundaţiei Universitare "Dunărea de Jos", Galaţi, 2004.

4. Oancea, N. *Metode numerice pentru profilarea sculelor, vol. I*, Universitatea "Dunărea de Jos", Galaţi 1980.

5. Oancea, N. *Metode numerice pentru profilarea sculelor, vol. II*., Universitatea "Dunărea de Jos", Galaţi 1982.

6. Oancea, N. *Metode numerice pentru profilarea sculelor, vol. VI.,* Universitatea "Dunărea de Jos", Galaţi 1998.

7. Oancea, N. şi Baicu, I. *Metode numerice pentru profilarea sculelor, vol. VIII,* Universitatea "Dunărea de Jos", 2002.

8. Oancea, N. şi Baicu, I. *Modeling of Surfaces Generations*. In: Analele Universităţii "Dunărea de Jos" din Galaţi, Fasc. V, Tehnologii în construcţia de maşini, anul XX (XXV)-2002, p. 48-45.

Algoritm pentru studiul angrenajului spiroidal

Rezumat

În lucrare, se propune un model, cu caracter de generalitate, pentru studiul suprafeţelor reciproc înfăşurătoare, utilizând teoremele fundamentale şi complementare ale teoriei înfăşurării suprafeţelor. Prin particularizări, modelul poate fi privit ca reprezentând o multitudine de tipuri de angrenaje cunoscute: angrenajul melcat, angrenajul spiroidal, angrenajul cu axe paralele, angrenajul conic etc. Se prezintă o soluţie privind angrenajul spiroidal cilindric.

Algorithme pour l'etude de l'engrenage spiroïdal

Résumé

Dans ce papier on presente un modèle, avec le caractère général, étudier des surfaces enveloppe, en utilisant des théorèmes fondamentaux et complémentaires d'envelopper des surfaces. Le modèle peut être considéré comme le fait de représenter une multitude de types connus d'engrenages. On présente l'engrenage spiroïdal.